Title
Multivalent ligands control stem cell behaviour in vitro and in vivo.

Journal
Nature nanotechnology, 8(11)

ISSN
1748-3387

Authors
Conway, Anthony
Vazin, Tandis
Spelke, Dawn P
et al.

Publication Date
2013-11-01

DOI
10.1038/nnano.2013.205

Peer reviewed

Published in final edited form as:

Nat Nanotechnol. 2013 November ; 8(11): 831–838. doi:10.1038/nnano.2013.205.

Multivalent ligands to control stem cell behaviour in vitro and in vivo

Anthony Conway[1], **Tandis Vazin**[1,2], **Dawn P. Spelke**[2], **Nikhil A. Rode**[3], **Kevin E. Healy**[2,3], **Ravi S. Kane**[4], and **David V. Schaffer**[1,2]

[1]Department of Chemical and Biomolecular Engineering, University of California Berkeley, Berkeley, California, USA

[2]Department of Bioengineering, University of California Berkeley, Berkeley, California, USA

[3]Department of Material Science and Engineering, University of California Berkeley, Berkeley, California, USA

[4]Department of Chemical and Biological Engineering, Rensselaer Polytechnic Institute, Troy, NY, USA

Abstract

There is broad interest in designing nanostructured materials that can interact with cells and regulate key downstream functions[1–7]. In particular, materials with nanoscale features may enable control over multivalent interactions, which involve the simultaneous binding of multiple ligands on one entity to multiple receptors on another and are ubiquitous throughout biology[8–10]. Cellular signal transduction of growth factor and morphogen cues that play critical roles in regulating cell function and fate often begins with such multivalent binding of ligands, either secreted or cell-surface tethered, to target cell receptors, leading to receptor clustering[11–18]. Cellular mechanisms that orchestrate ligand-receptor oligomerisation are complex, however, and the capacity to control multivalent interactions and thereby modulate key signaling events within living systems is therefore currently very limited. Here we demonstrate the design of potent multivalent conjugates that can organise stem cell receptors into nanoscale clusters and control stem cell behaviour *in vitro* and *in vivo*. The ectodomain of ephrin-B2, normally an integral membrane protein ligand, was conjugated to a soluble biopolymer to yield multivalent nanoscale conjugates that potently induced signaling in neural stem cells and promoted their neuronal differentiation both in culture and within the brain. Super-resolution microscopy analysis yielded insights into the organisation

Correspondence should be addressed to D.V.S. (schaffer@berkeley.edu).

AUTHOR CONTRIBUTIONS

A.C. performed all of the experiments and analyzed all data. A.C. and D.V.S. designed the ephrin-B2 experiments and wrote the manuscript. T.V., A.C., and D.V.S. designed the ephrin-B1 experiments. D.P.S. cloned the EphB4-Dendra2 retroviral vector. N.R. conducted the SEC-MALS experiment. K.E.H. and R.S.K. provided critical feedback on the manuscript.

COMPETING FINANCIAL INTERESTS

K.E.H. is an inventor of intellectual property related to HA bioconjugates. T.V. is an inventor of intellectual property related to dopaminergic differentiation of hESCs using SPIE.

Supplementary information accompanies this paper at www.nature.com/naturenanotechnology.

of receptor-ligand clusters at the nanoscale. We also found that synthetic multivalent conjugates of ephrin-B1 strongly enhanced human embryonic and induced pluripotent stem cell differentiation into functional dopaminergic neurons. Multivalent bioconjugates thus represent powerful tools and potential nanoscale therapeutics for controlling the behaviour of target stem cells *in vitro* and *in vivo*.

Adult neural stem cells (NSC) are an important class of therapeutically relevant cells, persist in specific regions of the mammalian brain, and have the capacity to generate new neurons and glia throughout life[19]. In addition, human pluripotent stem cells (hPSCs) – which include human embryonic stem cells (hESCs) and induced pluripotent stem cells (hiPSCs) – have the capacity to differentiate into all cells of the adult body and therefore offer broad potential for cell replacement therapy and modeling human disease. We recently found that ephrin-Eph signaling regulates both the neuronal differentiation of adult hippocampal NSCs[19] and the differentiation of hESCs into dopaminergic neurons[20], cells lost in Parkinson's disease. The design of molecules that regulate ephrin-Eph signaling in NSCs and hPSCs could therefore advance both basic biology and therapeutic applications.

To create synthetic multivalent ligands with potentially high potencies, recombinantly produced ephrin-B2 extracellular domain was conjugated at a range of stoichiometries to high molecular weight hyaluronic acid (HA) – a well-characterised biopolymer present throughout the body and in particular within the brain – using EDC/Sulfo-NHS chemistry, as previously described[21] (Fig. 1a,b). Valencies of the resulting ~100 nm polymeric conjugates[22] – estimated using a bicinchoninic acid (BCA) assay and further quantified with size exclusion chromatography coupled with multi-angle light scattering (SEC-MALS) (Fig. 1c) – ranged from 2 to 25 ephrin molecules per HA chain in this synthesis.

Based on the recently discovered role of ephrin-B2 signaling in regulating neuronal lineage commitment of adult NSCs[19], we investigated the activity of the multivalent conjugates in NSC culture. At a given concentration of ephrin-B2 ectodomain molecules, increasing the valency of HA:Ephrin-B2 conjugates progressively elevated neuronal differentiation (Fig. 1d,e). Strikingly, compared to antibody-clustered ligand, the 1:22, 1:12, and 1:8 valency conjugates induced similar levels of neuronal differentiation at 37-, 26-, and 9-fold lower protein concentrations, respectively. Thus, in contrast to the current, standard antibody-clustered form, whose low potency necessitates high concentrations, the multivalent ligands are potent agonists, with potentially reduced cost. Next, the addition of monomeric ephrin-B2 in tenfold molar excess to Fc-ephrin-B2 wells blocked differentiation, further establishing that ephrin clustering is required for activity. Finally, the results were further validated by quantifying mRNA levels of the neuronal marker *Tubb3* (Fig. 1f).

We next compared the ability of natural and synthetic ligands to cluster Eph receptors. Since ephrin-B2 presented from astrocytes regulates the neuronal differentiation of adult NSCs[19], we analyzed ephrin-Eph localisation on NSCs in contact with hippocampal astrocytes. Punctate staining of both ephrin-B2 and its receptor EphB4 was observed at cell-cell junctions (Fig. 2a), and co-localisation of the ligand and receptor was also observed at cell-cell contacts in the subgranular zone (SGZ) of the adult hippocampus (Fig. 2b), where NSCs reside[19].

We then analyzed whether the multivalent conjugates could emulate this natural process of receptor-ligand assembly. Fluorescently-labeled ephrin-B2 conjugates were synthesised and incubated with NSCs, at 4 °C to block endocytosis. EphB4 localisation was diffuse across the cell membrane in the absence of ephrin-B2 or with low ratio conjugates, whereas EphB4 puncta were observed in the presence of highly multivalent conjugates or antibody-clustered ligand (Fig. 2c). Additionally, while low ephrin-B2 valency conjugates yielded fewer and smaller EphB4 clusters than antibody-clustered ligand, high valency conjugates showed more (Fig. 2d), larger (Fig. 2e), and more intense (Fig. 2f) EphB4 clusters in close proximity (within the ~250 nm resolution limit of light microscopy) to fluorescently tagged ephrin-B2. Ligand multivalency therefore modulates both the number and the size of receptor clusters. In addition, we generated conjugates from ephrin-B2 protein recombinantly produced in mammalian cells and observed similar cell surface binding, indicating different protein expression systems result in similar downstream conjugate binding (Supplementary Fig. 1a).

Next, to explore the effect of ligand spacing on NSC differentiation and cell receptor clustering, monodisperse hyaluronic acid (HA) molecules of varying molecular weights were conjugated with recombinant ephrin-B2 extracellular domains tagged with fluorescent Alexa Fluor 647 molecules. Reactions were performed such that the polymers of varying molecular weights were linked to an equal number of fluorescently-tagged proteins, with the lower molecular weight conjugate containing an apparently saturated number of ephrin ligands (1:5 HA:Ephrin-B2 final molar ratio). The high molecular weight conjugates thus had greater inter-ligand spacing than lower molecular weight conjugates. After 6 days of culture, lower molecular weight conjugates induced significantly higher neuronal differentiation from NSCs, and higher molecular weight conjugates showed significantly less differentiation, compared to antibody-clustered Fc-ephrin-B2 (Fig. 2g). Inter-ligand spacing thus modulates conjugate activity.

Since standard fluorescence microscopy cannot accurately analyze the clustering properties of different molecular weight conjugates, we applied recently-developed super-resolution microscopy approaches to image receptor clusters on NSCs at 16 nm resolution. We generated a NSC line expressing an EphB4-Dendra2[23] fusion protein for photoactivatable localisation microscopy (PALM)[24], which was combined with direct stochastic optical resolution microscopy (dSTORM)[25] of Alexa Fluor 647-tagged HA:Ephrin-B2 conjugates (Fig. 2h). A single EphB4 and Ephrin-B2 signal were considered co-localised (and thus the molecules likely bound) when found to lie within the 16 nm resolution of the technique, corresponding to a single pixel in the images. We first analyzed receptor-ligand clusters for NSCs co-cultured with astrocytes and verified the existence of punctate staining at astrocyte-NSC junctions (Supplementary Fig. 2a), and co-localisation of ephrin-B2 with EphB4 was significantly more prevalent on NSCs when in contact with astrocytes (Supplementary Fig. 2b).

We next analyzed clusters generated by multivalent conjugates. In the absence of ligand, EphB4 was patchy but diffuse. However, after incubation of conjugates with cells for 4 hours at 4 °C, the spacing between ephrin-B2 ligands that co-localised with EphB4 was significantly lower for the lower molecular weight HA conjugates (Fig. 2i). Furthermore, conjugates with closer ephrin-B2 inter-ligand spacing formed significantly more EphB4

clusters, which were also denser (i.e. higher number of co-localised EphB4-ephrin-B2 signals per nm^2), compared to conjugates with larger ephrin-B2 inter-ligand spacing (Fig. 2j–l). Consequently, the shorter polymer conjugates resulted in more ligand-bound EphB4 molecules per cell (Fig. 2m) and per individual cluster (Fig. 2n). Since the number of co-localised EphB4-ephrin-B2 signals was larger than the valency of a single conjugate, each receptor-ligand cluster involved multiple bound conjugates, consistent with reports of lateral Eph receptor clustering[26]. Super-resolution imaging also confirmed that multivalent ligands produced in different expression systems yielded indistinguishable numbers, sizes, and densities of ligand-receptor clusters (Supplementary Fig. 3a–d). Modulating inter-ligand spacing can thus control the number of clusters per cell and number of receptors per cluster, potentially due to entropic effects associated with the conjugate's polymer backbone[27], and thereby control stem cell differentiation.

Ephrin-B2 induces neuronal differentiation by downstream activation of the transcriptional co-activator β-catenin[19]. Western blotting indicated that higher valency conjugate activated β-catenin significantly more than antibody-clustered Fc-ephrin or HA alone (Fig. 3a,b). Furthermore, a β-catenin responsive promoter-reporter construct showed a higher quantitative level of activation with increasing valency, which at a 1:31 valency was substantially greater than antibody-clustered Fc-ephrin-B2 (Fig. 3c). Finally, β-catenin drives neuronal differentiation via transcriptional activation of the proneural transcription factor *NeuroD1*[19], and multivalent ephrin-B2 conjugates with increasing valency again progressively induced higher levels of expression of this important target (Fig. 3d).

Multivalent conjugates may have strong utility not only *in vitro* but also *in vivo*. To investigate the latter, multivalent ephrin-B2 was administered into the hippocampal region of the adult rodent brain to analyze its ability to modulate endogenous stem cell function. Bromodeoxyuridine (BrdU) was administered to label dividing cells, followed by stereotactic injection of the ephrin-B2 conjugate or controls (Fig. 4a). After 5 days, the fractions of newly born cells ($BrdU^+$) that had differentiated into neurons (DCX^+) was quantified in tissue sections[19]. Antibody-clustered ligand showed a modest 20% increase over the uninjected or vehicle-injected HA control brains at the ephrin levels administered; however, the same number of ephrin-B2 domains incorporated into the highly multivalent conjugate yielded a substantial 60% increase in neurogenesis in the brain (Fig. 4b,c). These data demonstrate that nanoscale organisation in the presentation of this ligand greatly enhances its ability to elicit cellular responses both *in vitro* and *in vivo*.

We next assessed the generality of this approach with both hESCs and hiPSCs. Vazin *et al*. showed that unclustered ephrin-B1 – in combination with soluble stromal cell-derived factor-1 (SDF-1), pleiotrophin (PTN), and IGF-2, a blend known as SPIE – enhanced hESC differentiation into midbrain dopaminergic neurons[20], which are being considered as cell replacement therapies for Parkinson's disease[28]. By analogy with ephrin-B2, we synthesised multivalent ephrin-B1 conjugates. Using conjugates of varying valency, along with the other components of SPIE, hESCs were first differentiated within embryoid bodies and then toward dopaminergic neurons for 14–18 days (Fig. 5a). After 15 days, transcripts for the midbrain-specific marker *En1* increased with higher valency (Fig. 5b), and QPCR showed

that both the pan-neuronal marker*Tubb3* and the dopaminergic marker *TH* progressively increased with conjugate valency (Fig. 5c).

Immunostaining was then conducted to quantify cell differentiation into a dopaminergic lineage. After 15–18 days of differentiation in ephrin post-embryoid body formation, hESC-derived cultures exhibited substantially higher proportions of cells expressing pan-neuronal (Map2) and the dopaminergic neuron (TH) markers with increasing conjugate valency, compared to antibody-clustered ephrin-B1 (Fig. 5d–f). Similar results were achieved with hiPSCs (Supplementary Fig. 4a,b). Since contaminating cells within dopaminergic grafts have been associated with adverse events in clinical trials[29], approaches to improve dopaminergic neuron purity are significant. Finally, to assess the functional properties of the differentiated dopaminergic neurons, levels of the neurotransmitter dopamine were measured, either in conditioned medium or upon addition of KCl to induce synaptic neurotransmitter release. Dopamine levels increased with increasing valency and were greater with highly multivalent conjugates than antibody-clustered groups (Fig. 5g), consistent with the observed higher dopaminergic differentiation levels observed with the conjugates.

As an initial assessment of how multivalent ephrin affects differentiating cultures, at various times over 14 days cells received a 24 hour pulse of bromodeoxyuridine (BrdU) to quantify DNA synthesis. Cells with multivalent ephrin-B1 remained mitotically active longer than with unclustered ephrin-B1 or no SPIE factors, indicating that enhanced proliferation of intermediate neuronal progenitors may increase the number of dopaminergic neurons in fully differentiated cultures (Fig. 5h). These results indicate that ephrin effects on dopaminergic differentiation are complex, and the multivalent conjugates will enable future mechanistic investigation of the role of this signaling system in dopaminergic neuron generation.

This study demonstrates that multivalency greatly enhances the bioactivity of ligands that regulate stem cell behaviour, and multivalent conjugates thus have utility for mechanistic investigation in both stem cell and developmental biology. Studying the mechanistic role of receptor complex assembly in cell-cell contact dependent Delta-Notch[11], c-kit[12], Fas ligand[13], and Flt ligand[14] signaling – as well as matrix-binding fibroblast growth factor (FGF)[15], transforming growth factor-β (TGF-β)[16], Hedgehogs (Hh)[17], vascular endothelial growth factor (VEGF)[18] signaling – and other signaling systems could greatly benefit from nanoscale synthetic ligands that potently activate receptors in a biomimetic fashion. For example, the effects of many receptor-ligand complex properties – including the number of receptor clusters per cell, cluster size, ligand scaffold, inter-receptor distance within an oligomer, and induced heteroligomerisation of different receptors into the same cluster – on biological activity can now be systematically varied and studied *in vitro* or *in vivo*. Furthermore, nanoscale multivalent conjugates could potentially activate these systems more potently, and thus less expensively. Finally, this platform has biotechnological and biomedical applications, including in cell culture systems, bioactive materials, and drug delivery technologies.

METHODS

Recombinant protein production, purification, and bioconjugation

Murine ephrin-B2 ectodomain sequence (amino acids 31–227) was amplified from the plasmid pcDNA3.1-ephrin-B2-hFc (a kind gift from T. Miyamoto, Keio University), and human ephrin-B1 ectodomain sequence (amino acids 28–237) was amplified from pALTER-MAX (a kind gift from H. Sugimura, Hamamatsu University). A C-terminal hexahistidine tag and cysteine were added during PCR, followed by insertion into the bacterial expression plasmid pBAD. Protein was expressed in bacteria and purified as previously described[21]. Protein purity was assessed by confirmation of a single band following SDS-PAGE. Purified ephrin-B2 or ephrin-B1 was conjugated to 800 kDa hyaluronic acid (HA) (Genzyme) or to a range of monodisperse molecular weight HAs (Hyalose) through a two-step reaction using carbodiimide chemistry at the HA carboxylate group and a maleimide reaction at the protein C-terminal cysteine[21]. In the first step, 3,3′-*N*-(ε-Maleimidocaproic acid) hydrazide (EMCH, Pierce, 1.2 mg/mL), *N*-hydroxysulfosuccinimide (Sulfo-NHS, Pierce, 2.8 mg/mL), and 1-ethyl-3-(3-dimethylaminopropyl) carbodiimide hydrochloride (EDC, Pierce, 10 mg/mL) were added to a 3 mg/mL solution of HA in 0.1 M 2-(*N*-morpholino)ethanesulfonic acid (MES) (Sigma) buffer pH 6.5 and allowed to react at 4 °C for 4 hours. The solution was then dialyzed into pH 7.0 PBS containing 10% glycerol and 2 mM EDTA. Recombinant ephrin-B2 or ephrin-B1 was reduced using Tris(2-carboxyethyl)phosphine hydrochloride (TCEP) (Pierce) in 200-fold molar excess and reacted at 4 °C for 5 minutes. Activated HA-EMCH was then added at desired molar ratios with reduced ephrin-B2 or ephrin-B1 and allowed to react at 4 °C overnight. The ephrin-conjugated HA was dialyzed with 100 kDa MWCO tubing (Spectrum Labs) in pH 7.0 PBS containing 2 mM EDTA to remove unreacted ephrin. Purified ephrin and HA-conjugated ephrin protein concentrations were measured using a BCA assay, and valencies were verified using SEC-MALS as previously described[21].

Antibody-clustered ephrin-B formation

To create clustered ephrin-B2 and ephrin-B1 complexes (Fc-ephrin-B), recombinant mouse ephrin-B/Fc chimera (R&D Systems) was incubated with goat anti-human IgG, Fc-fragment specific, (Jackson ImmunoResearch) antibody at a 1:9 ratio (w/w), which led to maximal activity of the resulting clusters (data not shown). After 90 min at 4 °C, complexes were used immediately.

Cell culture and differentiation

NSCs were cultured as previously described[30]. For differentiation studies, 8-well chamber slides were seeded with 2×10^4 cells per well in standard culture medium containing 0.1 ng/mL FGF-2. For the subsequent 6 days, ephrin-B2 was added at the desired molar concentration, and daily 50% media changes were performed. EphB4 cluster properties were quantified using ImageJ.

Immunostaining

Coronal brain sections (40 μm) were processed, stored, and stained as previously described[31]. Sections were then mounted on glass slides, and either stereological analysis (Stereo Investigator, MBF Biosciences) or confocal microscopy (LSM 710, Zeiss) was performed. In short, using an optical fractionator method, $BrdU^+$ and DCX^+ cells were counted in a Systematic Randomly Sampled (SRS) set of unbiased virtual volumes inside the subgranular zone and granular cell layer of both the left and right sides of the hippocampus. An estimate of the total number of $DCX^+/BrdU^+$ cells in the hippocampus was then generated.

Super-resolution microscopy

Cultures incubated with fluorescent conjugate were fixed and in some cases immunostained with Alexa 647 or Alexa 488 tagged antibodies, then incubated with 100 nm Tetraspeck fluorescent beads (Life Technologies) in PBS at a 1:2000 (v/v) dilution to act as reference points during imaging to later use for drift correction in image reconstruction. The sample coverslips were then placed in an Attofluor cell chamber (Life Technologies) and incubated in cold, freshly made pH 8.0 buffer containing 100 mM cysteamine (Sigma), 50 mM Tris, 10 mM NaCl, 10% (wt/v) glucose, 560 μg/mL glucose oxidase (Sigma), and 34 μg/mL catalase (Sigma). Using a microscope (TE2000, Nikon) with adaptive optics for 3D localisation[32], a piezoelectric stage, and highly inclined thin illumination capability[33], photoactivatable localisation microscopy (PALM)[24] was performed to detect EphB4-Dendra2[23] simultaneously with direct stochastic optical reconstruction microscopy (dSTORM)[25] to detect Alexa Fluor 647-tagged ephrin-B2 conjugates, as previously described[24–25]. Sub-diffraction limit images were then reconstructed using QuickPALM and quantified using ImageJ. To detect individual ephrin-B2 signals that co-localised with EphB4 signals, individual channel intensities were maximised, merged, then made into a binary image to display only co-localised pixels, indicating a proximity of signals within 16 nm. EphB4 or ephrin-$B2^+$ clusters were defined as any grouping of 10 or more positive pixels within a total diameter of 10 to 100 pixel widths.

Statistical analysis

Statistical significance of the results was determined using an ANOVA and multiple means comparison function (Tukey-Kramer method) in MATLAB with an alpha level of 0.05. All error bars are reported in s.d. from the mean, with $n = 3$ unless otherwise noted.

Supplementary Material

Refer to Web version on PubMed Central for supplementary material.

Acknowledgments

We thank Agnieszka Ciesielska (Bankiewicz Lab, UCSF) for help with HPLC analysis of dopamine and Jacob Martin (RPI) for suggestions regarding the synthesis of multivalent ligands based on monovalent hyaluronic acid scaffolds. This work was supported by NIH R21 EB007295 and California Institute for Regenerative Medicine grant RT2-02022. A.C. and T.V. were partially supported by training grant fellowships from CIRM (T1-00007). D.P.S. was partially supported by an NSF Graduate Research Fellowship and a training grant fellowship from CIRM (TG2-01164).

References

1. Jiang W, Kim BY, Rutka JT, Chan WC. Nanoparticle-mediated cellular response is size-dependent. Nat Nanotechnol. 2008; 3:145–150. [PubMed: 18654486]
2. Mannix RJ, et al. Nanomagnetic actuation of receptor-mediated signal transduction. Nat Nanotechnol. 2008; 3:36–40. [PubMed: 18654448]
3. McMurray RJ, et al. Nanoscale surfaces for the long-term maintenance of mesenchymal stem cell phenotype and multipotency. Nat Mater. 2011; 10:637–644. [PubMed: 21765399]
4. Ng QK, et al. Engineering clustered ligand binding into nonviral vectors: alphavbeta3 targeting as an example. Mol Ther. 2009; 17:828–836. [PubMed: 19240693]
5. Maheshwari G, Brown G, Lauffenburger DA, Wells A, Griffith LG. Cell adhesion and motility depend on nanoscale RGD clustering. J Cell Sci. 2000; 113:1677–1686. [PubMed: 10769199]
6. Lee LA, et al. Multivalent Ligand Displayed on Plant Virus Induces Rapid Onset of Bone Differentiation. Mol Pharm. 2012; 9:2121–2125. [PubMed: 22646283]
7. Petrie TA, et al. Multivalent integrin-specific ligands enhance tissue healing and biomaterial integration. Sci Transl Med. 2010; 2:45ra60.
8. Mammen M, Choi SK, Whitesides GM. Polyvalent Interactions in Biological Systems: Implications for Design and Use of Multivalent Ligands and Inhibitors. Angew Chem Int Ed. 1998; 37:2754–2794.
9. Kiessling LL, Gestwicki JE, Strong LE. Synthetic multivalent ligands in the exploration of cell-surface interactions. Curr Opin Chem Biol. 2000; 4:696–703. [PubMed: 11102876]
10. Vance D, Shah M, Joshi A, Kane RS. Polyvalency: a promising strategy for drug design. Biotechnol Bioeng. 2008; 101:429–434. [PubMed: 18727104]
11. Artavanis-Tsakonas S, Rand MD, Lake RJ. Notch signaling: cell fate control and signal integration in development. Science. 1999; 284:770–776. [PubMed: 10221902]
12. Broudy VC, Lin NL, Buhring HJ, Komatsu N, Kavanagh TJ. Analysis of c-kit receptor dimerization by fluorescence resonance energy transfer. Blood. 1998; 91:898–906. [PubMed: 9446650]
13. Holler N, et al. Two adjacent trimeric Fas ligands are required for Fas signaling and formation of a death-inducing signaling complex. Mol Cell Biol. 2003; 23:1428–1440. [PubMed: 12556501]
14. Barleon B, et al. Mapping of the sites for ligand binding and receptor dimerization at the extracellular domain of the vascular endothelial growth factor receptor FLT-1. J Biol Chem. 1997; 272:10382–10388. [PubMed: 9099677]
15. Ye S, et al. Structural basis for interaction of FGF-1, FGF-2, and FGF-7 with different heparan sulfate motifs. Biochemistry. 2001; 40:14429–14439. [PubMed: 11724555]
16. Haudenschild DR, et al. Enhanced activity of TGF-beta1 bound to cartilage oligomeric matrix protein. J Biol Chem. 2011; 286:43250–43258. [PubMed: 21940632]
17. Chang SC, Mulloy B, Magee AI, Couchman JR. Two distinct sites in sonic Hedgehog combine for heparan sulfate interactions and cell signaling functions. J Biol Chem. 2011; 286:44391–44402. [PubMed: 22049079]
18. Krilleke D, Ng YS, Shima DT. The heparin-binding domain confers diverse functions of VEGF-A in development and disease: a structure-function study. Biochem Soc Trans. 2009; 37:1201–1206. [PubMed: 19909247]
19. Ashton RS, et al. Astrocytes regulate adult hippocampal neurogenesis through ephrin-B signaling. Nat Neurosci. 2012; 15:1399–1406. [PubMed: 22983209]
20. Vazin T, et al. A novel combination of factors, termed SPIE, which promotes dopaminergic neuron differentiation from human embryonic stem cells. PLoS One. 2009; 4:e6606. [PubMed: 19672298]
21. Wall ST, et al. Multivalency of Sonic hedgehog conjugated to linear polymer chains modulates protein potency. Bioconjug Chem. 2008; 19:806–812. [PubMed: 18380472]
22. Pollock JF, Ashton RS, Rode NA, Schaffer DV, Healy KE. Molecular characterization of multivalent bioconjugates by size-exclusion chromatography with multiangle laser light scattering. Bioconjug Chem. 2012; 23:1794–1801. [PubMed: 22794081]

23. Gurskaya NG, et al. Engineering of a monomeric green-to-red photoactivatable fluorescent protein induced by blue light. Nature Biotechnology. 2006; 24:461–465.
24. Betzig E, et al. Imaging intracellular fluorescent proteins at nanometer resolution. Science. 2006; 313:1642–1645. [PubMed: 16902090]
25. van de Linde S, et al. Direct stochastic optical reconstruction microscopy with standard fluorescent probes. Nat Protoc. 2011; 6:991–1009. [PubMed: 21720313]
26. Pasquale EB. Eph receptor signalling casts a wide net on cell behaviour. Nat Rev Mol Cell Biol. 2005; 6:462–475. [PubMed: 15928710]
27. Kane RS. Thermodynamics of multivalent interactions: influence of the linker. Langmuir. 2010; 26:8636–8640. [PubMed: 20131760]
28. Lindvall O. Dopaminergic neurons for Parkinson's therapy. Nat Biotechnol. 2012; 30:56–58. [PubMed: 22231097]
29. Politis M, et al. Serotonergic neurons mediate dyskinesia side effects in Parkinson's patients with neural transplants. Sci Transl Med. 2010; 2:38ra46.
30. Lai K, Kaspar BK, Gage FH, Schaffer DV. Sonic hedgehog regulates adult neural progenitor proliferation in vitro and in vivo. Nat Neurosci. 2003; 6:21–27. [PubMed: 12469128]
31. Kempermann G, Kuhn HG, Gage FH. More hippocampal neurons in adult mice living in an enriched environment. Nature. 1997; 386:493–495. [PubMed: 9087407]
32. Zawadzki RJ, et al. Adaptive-optics optical coherence tomography for high-resolution and high-speed 3D retinal in vivo imaging. Opt Express. 2005; 13:8532–8546. [PubMed: 19096728]
33. Tokunaga M, Imamoto N, Sakata-Sogawa K. Highly inclined thin illumination enables clear single-molecule imaging in cells. Nat Methods. 2008; 5:159–161. [PubMed: 18176568]

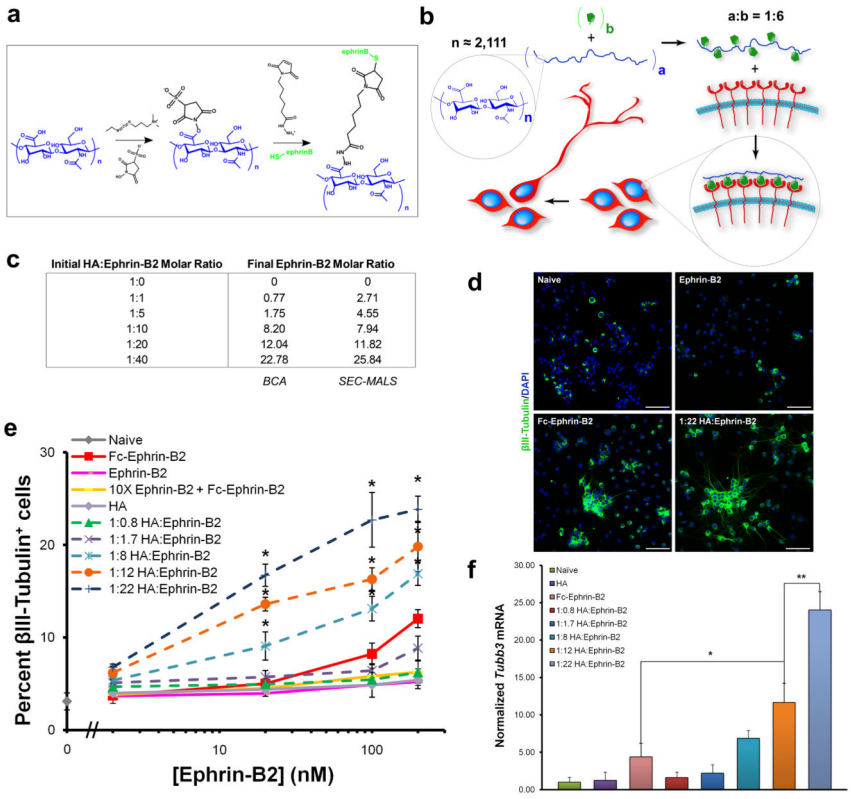

Figure 1.

Multivalent ephrin-B2 enhances neuronal differentiation of NSCs *in vitro*. **(a)** Chemical schematic of HA functionalisation and recombinant protein conjugation. **(b)** Schematic of protein (green) conjugation to 800 kDa linear HA (blue) and subsequent clustering of receptors (red) upon introduction to cells, inducing neuronal differentiation. The molecular structure represents an HA monomer subunit, of which there are approximately 2,111 (n) in 800 kDa HA. The ratio of a:b represents the valency of HA molecules to covalently-bound protein subunits. **(c)** Comparative BCA vs. SEC-MALS analysis for a range of ephrin-B2 bioconjugate valencies. **(d)** Representative images of cultured NSCs differentiated for 6 days in media alone (naïve) or in the presence of unclustered ephrin-B2, antibody clustered Fc-ephrin-B2, or multivalent 1:22 HA:Ephrin-B2, then immunostained for the neuronal marker βIII-Tubulin (green) and total nuclei (blue). Scale bars, 100 μm. **(e)** Quantification of the total fraction of neurons after 6 days of NSC differentiation in the presence of ephrin-B2 conjugates (dashed lines) or controls (solid lines), as assessed by immunostaining. * $P <$ 0.05 compared to Fc-ephrin-B2 at corresponding ephrin-B2 concentrations. **(f)** qPCR for the neuronal transcript *Tubb3* after 6-day differentiation. * $P = 0.0159$, ** $P = 0.0037$. All error bars represent s.d. from the mean.

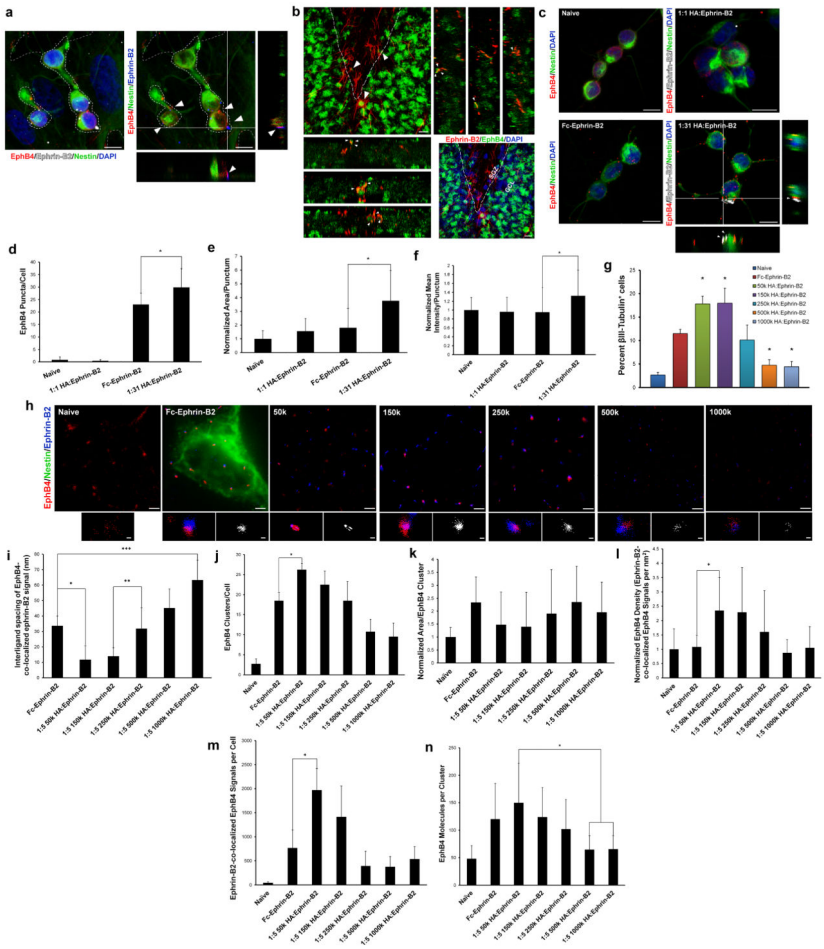

Figure 2.

Multivalent ephrin-B2 enhances receptor clustering. **(a)** Representative image of EphB4 (red) and ephrin-B2 (white) clustering (white arrow heads) on the surface of NSCs (stained with the neural stem cell marker nestin, pseudo-coloured green, and outlined with white dashed lines) and hippocampal astrocytes (edges outlined with grey dashed lines), respectively, in co-culture. All cell nuclei are shown in blue. Scale bars, 10 μm. **(b)** EphB4 (green) receptor clustering (white arrow heads) on the surface of multiple cells in the hippocampal subgranular zone (SGZ) in contact with ephrin-B2^{+} astrocytes (red). All cell nuclei are shown in blue. Scale bars, 10 μm. **(c)** Representative images of NSCs incubated with fluorescently labeled ephrin-B2 bioconjugates (white) for 4 hours at 4 °C and immunostained for their cognate receptor EphB4 (red), the neural stem cell marker nestin (green), and total nuclei (blue). White arrow heads indicate ephrin-B2/EphB4 co-localization. Scale bars, 10 μm. **(d)** Quantification of total number of EphB4 puncta per cell after incubation with ephrin-B2, either antibody-clustered or a new preparation of conjugate. * $P = 0.024$ by ANOVA, n ≥ 10. **(e)** Normalised area per EphB4 punctum after incubation with ephrin-B2. * $P = 5.33\times10^{-9}$ by ANOVA, n ≥ 62. **(f)** Normalised mean EphB4 signal intensity per punctum after incubation with ephrin-B2. * $P = 0.001$ by ANOVA, n ≥ 62. **(g)** Immunostaining quantification of the total fraction of neurons after 6 days of NSC

differentiation in the presence of Alexa Fluor 647 tagged ephrin-B2 conjugates of varying HA backbone molecular weight and antibody-clustered Fc-ephrin-B2 control, all at 200 nM protein concentration. * $P < 0.02$ compared to Fc-ephrin-B2. **(h)** Representative reconstructed super-resolution images of EphB4-Dendra2 (red) NSCs incubated with fluorescently labeled ephrin-B2 bioconjugates (blue) for 4 hours at 4 °C and then immunostained for the neural stem cell marker nestin (green). Magnified images of representative EphB4/ephrin-B2 clusters are shown below whole cell images, with co-localised pixels indicated in white. Large scale bars, 1000 nm; small scale bars, 100 nm. **(i)** Quantification of average inter-ligand spacing between individual ephrin-B2 signals that co-localised with EphB4, with a constant value of 16 nm per pixel. * $P = 1.80\times10^{-6}$. ** $P = 0.0006$. *** $P = 1.22\times10^{-6}$. **(j)** Quantification of total number of EphB4 clusters per cell after incubation with fluorescent ephrin-B2. * $P = 0.0009$. **(k)** Normalised area per EphB4 cluster after incubation with fluorescent ephrin-B2. * $P = 5.33\times10^{-9}$. **(l)** Normalised number of co-localised EphB4-ephrin-B2 signals per nm^2 after incubation with ephrin-B2. * $P = 0.0015$. **(m)** Total number of co-localised EphB4-ephrin-B2 signals per cell after incubation with fluorescent ephrin-B2. * $P = 0.0064$. **(n)** Total number of EphB4 signals per cluster after incubation with fluorescent ephrin-B2. * $P < 0.05$. All error bars represent s.d. from the mean.

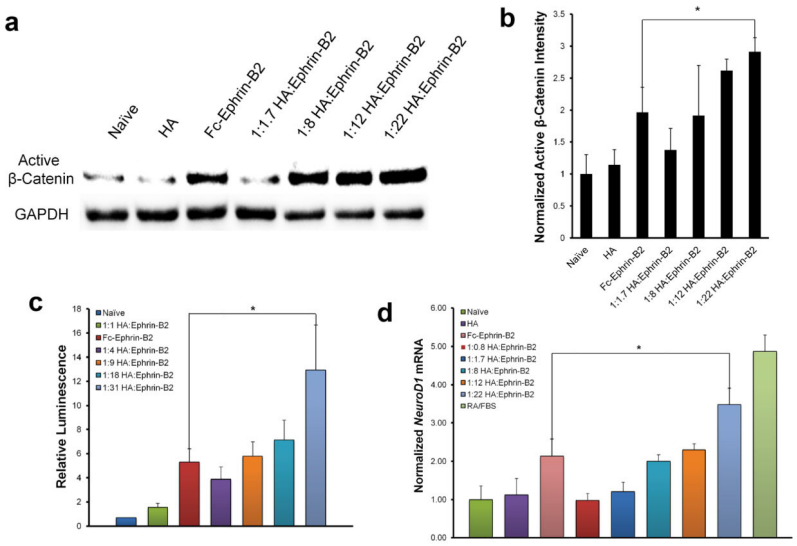

Figure 3.

Multivalent ephrin-B2 enhances downstream signaling. **(a)** Representative Western blot for active β-catenin and GAPDH, as a loading control, in NSC lysate after 24 hour incubation with ephrin-B2 bioconjugates. **(b)** Average levels of β-catenin activation normalised to GAPDH in n=3 blots. * $P = 0.0217$. **(c)** Quantification of β-catenin activation in NSCs after 24-hour incubation with fluorescently labeled ephrin-B2 bioconjugates at 37 °C, as assessed by upregulation of the transgenic luciferase reporter for β-catenin activity. * $P = 0.0267$. **(d)** qPCR for the intermediate transcriptional target of neurogenesis *NeuroD1* after 6 day differentiation. The RA/FBS group is described in detail in the Methods section. * $P = 0.0192$. All error bars represent s.d. from the mean.

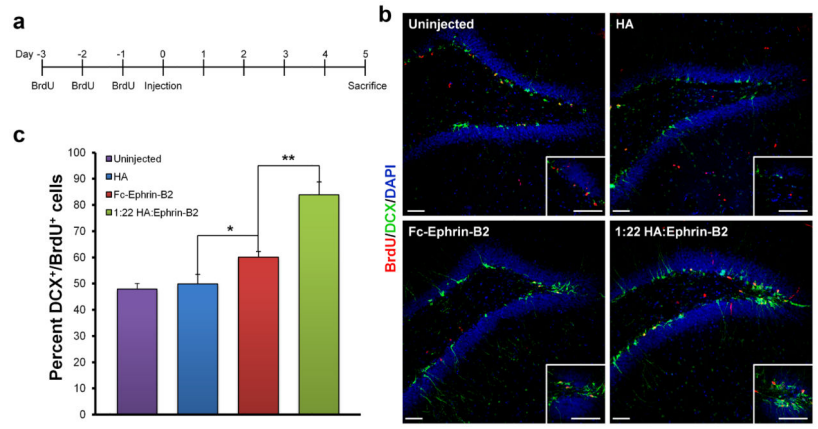

Figure 4.

Multivalent ephrin-B2 enhances *in vivo* neurogenesis. **(a)** Schematic of experimental timecourse. **(b)** Representative image of adult rat hippocampal sections 5 days after stereotactic injections, immunostained for BrdU (red) to label dividing cells, DCX (green) to label immature neurons, and DAPI to stain nuclei (blue). Scale bars, 100 μm. **(c)** Quantification of the overall fraction of newborn hippocampal cells that underwent neuronal differentiation using stereological estimation. * $P = 0.0136$, ** $P = 0.0015$. All error bars represent s.d. from the mean.

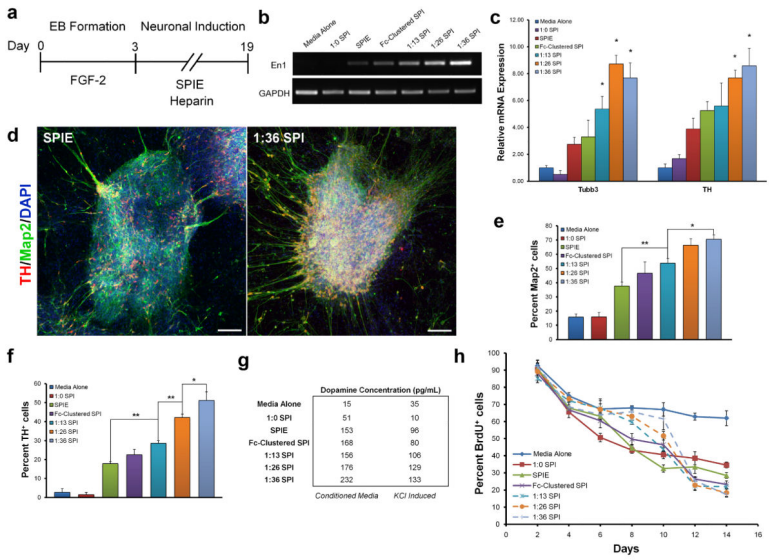

Figure 5.

Multivalent ephrin-B1 enhances neuronal and midbrain fates in differentiating hESCs. **(a)** Schematic of experimental timecourse. **(b)** RT-PCR analysis of midbrain-specific marker *En1* expression vs. control *G3PDH*, from HSF6 hESCs differentiated for 15 days post-embryoid body formation with ephrin-B1 conjugates or controls. **(c)** qPCR for the pan-neuronal marker*Tubb3* and the dopaminergic marker *TH* after 15-day differentiation of H1 hESCs with ephrin-B1 conjugates or controls. * $P < 0.05$ compared to SPIE for corresponding neuronal marker. **(d)** Representative images of cultured H1 hESCs differentiated for 18 days post-embryoid body formation with the SPI factors, heparin, and either Fc-ephrin-B1 or multivalent 1:36 HA:Ephrin-B1. Immunostaining for total neurons (green), dopaminergic neurons (red), and total nuclei (blue). Scale bars, 100 μm. **(e)** Quantification of the fraction of total neurons after differentiation of H1 hESCs in the presence of ephrin-B1 conjugates or controls, as assessed by immunostaining. * $P = 0.0181$, ** $P = 0.0029$. **(f)** Quantification of the fraction of dopaminergic neurons after differentiation of H1 hESCs in the presence of ephrin-B1 conjugates or controls, as assessed by immunostaining. * $P = 0.0328$, ** $P = 0.0004$. **(g)** Quantification of the fraction of mitotic cells on various days over the 14 day course of HSF6 hESC differentiation in the presence of ephrin-B1 conjugates (dashed lines) or controls (solid lines). **(h)** Quantification of total dopamine levels in cultures of H1 hESCs differentiated for 4 weeks in the presence of ephrin-B1 conjugates or controls, as assessed by HPLC with electrochemical detection. All error bars represent s.d. from the mean.